Faraday Discussions

Accepted Manuscript

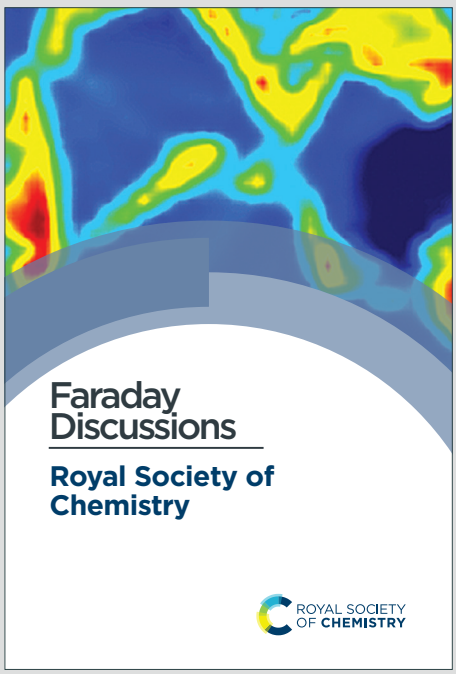

This article can be cited before page numbers have been issued, to do this please use: E. Tran, J. P. F. Ng, L. Dieval, S. Rouziere, P. Launois, M. S. P. Shaffer and A. Brandt-Talbot, *Faraday Discuss.*, 2025, DOI: 10.1039/D5FD00099H.

ROYAL SOCIETY OF CHEMISTRY

www.rsc.org/faraday_d

View Article Online
DOI: 10.1039/D5FD00099H

ARTICLE

Hot-drawing ionic liquid-spun lignin-poly(vinyl alcohol) fibres increases strength and polymer alignment

Received 6th June 2025,
Accepted 00th January 20xx

DOI: 10.1039/x0xx00000x

Enny Tran,[a,b†] Joanne Pui Fai Ng,[b†] Lucie Dieval,[c†] Stéphan Rouzière,[c] Pascale Launois,[c*] Milo S.P. Shaffer,[a,b*] and Agnieszka Brandt-Talbot[b*]

Lignin is an attractive raw material for low-cost sustainable carbon fibres, however, the resulting mechanical properties require improvement before they can be implemented in sustainable composite applications. The mechanical properties of conventional polyacrylonitrile-derived carbon fibres depend critically on the molecular alignment in the precursor polymer fibres and retention of the alignment through subsequent thermal treatments. In this study, alignment was induced in high lignin content fibres wet-spun from a low-cost ionic liquid water mixture by employing similar hot-drawing methods. 75/25 wt%/wt% lignin-poly(vinyl alcohol) (lignin-PVA) fibres were continuously wet-spun from a solvent containing *N,N*-dimethylbutylammonium hydrogen sulfate [DMBA][HSO_4] with 40% water, with deionised water used as the coagulant. Hot-drawn fibres with high draw ratios of up to 20 were generated at 180°C. By careful selection of the initial extrusion diameter and the subsequent draw ratio, the influence of fibre diameter and draw ratio was systematically distinguished. The draw ratio was found to dominate the mechanical properties of the precursor fibres, while the fibre diameter was more significant after stabilisation. The precursor fibres that experienced the highest draw ratios had tensile strengths of 235-249 MPa (up to four times higher than the undrawn lignin-PVA fibres) and 7.5-8.2 GPa tensile modulus, while the fibre diameter was reduced from 64-106 µm to 15-23 µm. Wide-Angle X-ray Scattering (WAXS) studies showed that hot-drawing induced oriented crystalline PVA domains at high draw ratios. The crystallisation and orientation of PVA was lost during the slow oxidative stabilisation at 250°C, associated with a plateau at around 110 MPa tensile strength and 4 GPa tensile modulus for the stabilised lignin-PVA fibres. Improvements to the stabilisation aimed at retaining alignment are proposed.

Keywords: Hot-stretching, continuous fibre spinning, Kraft lignin, ionic liquids, WAXS, FTIR spectroscopy, mechanical properties

Introduction

Carbon fibres are high-value components in lightweight structural composites due to their exceptional mechanical strength and stiffness. Carbon fibre reinforced composites have applications in the aerospace and automotive industries, and for the construction of wind turbines, which will aid decarbonisation.[1] The majority of commercial carbon fibres are produced from the pyrolysis of fibres wet-spun from poly(acrylonitrile) (PAN) using expensive solvents such as dimethylformamide (DMF), dimethylacetamide (DMAc) or dimethyl sulfoxide (DMSO).[2] The precursor fibres undergo oxidative thermal stabilisation to cross-link the polymers before pyrolysis (carbonisation) and graphitisation.[2, 3] While PAN carbon fibres have excellent mechanical properties, wide-spread application is limited by the high cost of carbon fibre manufacturing. Generating the precursor fibre contributes to around 50% of the carbon fibre production cost.[4] Moreover, PAN is derived from fossil fuel feedstocks, which links the material to global warming. Alternative precursors made from renewable feedstocks are needed to obtain carbon fibres with improved sustainability and at reduced production cost, together with mechanical properties that are sufficient for target applications.[5-9] The United States Department of Energy has determined a target of 1.72 GPa tensile strength and 172 GPa tensile modulus at a price of <$10/kg for low-cost sustainable carbon fibres for general automotive applications, 50% below the $20/kg for standard modulus carbon fibres (3.5 GPa tensile strength and 230 GPa tensile modulus).[4, 10]

Carbon fibres can be produced from lignin, an abundant polymer present in wood biomass. Lignin is biosynthesised from cinnamic alcohols via radical polymerisation and has no defined repeating unit.[11] Technical lignins are available as a low-cost by-product of chemical pulping, which is focused on isolating wood cellulose for fibre and dissolving applications.[12, 13] They are typically complex mixtures of molecules whose specific structure varies with the botanical source and the extraction method. Kraft

[a] Department of Materials, Imperial College London, South Kensington Campus, London SW7 2AZ, United Kingdom
[b] Department of Chemistry, Molecular Sciences Research Hub (MSRH), Imperial College London, 82 Wood Lane, London W12 0BZ, United Kingdom
[c] Université Paris-Saclay, CNRS, Laboratoire de Physique des Solides, Orsay, 91405, France
† These authors contributed equally to the work.
* Corresponding author email addresses: pascale.launois@cnrs.fr, m.shaffer@imperial.ac.uk, agi@imperial.ac.uk
Supplementary Information available. See DOI: 10.1039/x0xx00000x

View Article Online
DOI: 10.1039/D5FD00099H

pulping is one of the two industrially applied chemical pulping processes, with Kraft cellulose pulp widely used in paper, hygiene and packaging applications. The Kraft lignin is typically incinerated during the recovery of the pulping chemicals but can be isolated from the black liquor using LignoBoost precipitation.[14] Valorising lignin into materials is a route towards product diversification for Kraft pulp mills and could increase revenue. Lignins have been spun into fibre-form either alone or, more often, blended with polymers.[15] Lignin precursor fibres can be produced by melt-spinning, wet-spinning or dry-spinning.[16, 17] When solvents are used for fibre formation during wet-spinning, the cost of the solvents is important, and a fibre-forming additive must be used as the intermolecular interactions in lignin are too weak to maintain integrity during coagulation, indicated by low solution viscosities. Yang *et al.* developed a low-cost approach to spinning high lignin content precursor fibres, with up to 90% lignin content. Partially acetylated poly(vinyl alcohol) (PVA) was employed as the fibre-forming additive, while a low-cost ionic liquid (IL) water mixture was used as the solvent and pure water as the coagulation (non-) solvent.[18] The ionic liquid is projected to cost around $1/kg, which is 3-5 times cheaper than PAN spinning solvents such as DMSO,[19, 20] with production cost estimated as $9.02 - $9.69/kg for ionosolv carbon fibre.[21] The morphology of the carbonised fibres was ideal (circular and smooth surfaces), however, the mechanical performance of the single filament carbon fibres in the proof-of-concept study was only around 0.45 GPa tensile strength and 40 GPa tensile modulus for Kraft softwood lignin-PVA fibres of 54-100 µm diameter. The mechanical properties are below the state-of-the-art reported for lignin carbon fibres, which is up to 2.45 GPa tensile strength and 279 GPa tensile modulus, between the DoE target and standard modulus carbon fibres (Table S1, Supplementary). The modest performance was expected given that the fibres were produced *via* a rotating bath method that did not permit tensioning after coagulation.

Fibre diameter is an important processing parameter that influences tensile strength, as it correlates with the defect size and density, factors which control brittle failure; commercial carbon fibres are typically only 5-10 µm in diameter.[22, 23] Molecular alignment is also critical to the performance of polymer fibres; in the case of carbon fibres, the orientation of the precursor molecules plays a major role in determining the alignment of the graphitic planes after carbonisation, which in turn influences mechanical performance, especially stiffness. Applying tension during fibre processing is a key tool to increase axial alignment, through both gel-drawing and hot-drawing steps, in addition to maintaining the alignment during the subsequent thermal transformations that convert the polymer precursor into carbon. The optimisation of these steps has been critical to the industrialisation of PAN carbon fibres, and the continued improvement in their properties. For example, stretching during the washing and high-temperature drawing process orients PAN along the direction of the fibre axis and is a significant factor for producing carbon fibres with excellent tensile properties.[24] Although more rarely applied, drawing also improves the mechanical properties of lignin-derived carbon fibres; Luo *et al.* showed that stretching melt-spun organosolv lignin fibres using controlled and increasing tensioning during a prolonged stabilisation process improved the average tensile strength of the carbonised fibres from 549 MPa to 2.12 GPa and the average tensile modulus from 48 GPa to 189 GPa.[25] Vaughan *et al.* combined stretching during stabilisation of a melt-spun blend of an organosolv lignin and a thermoplastic polyurethane with the application of UV-irradiation as a cross-linking agent, generating high stiffness lignin carbon fibres with 279 GPa tensile modulus.[26]

A variety of wet/hot-drawing processes are applied commercially to thermoplastic PVA fibres to reduce the fibre diameter, improve orientation and induce crystallisation, resulting in better mechanical properties.[27-30] Some examples are also known for lignin-PVA fibres. Föllmer *et al.* showed that the tensile strength of Kraft lignin-PVA (70/30 wt/wt%) fibres, wet-spun from DMSO into isopropanol, was increased from around 80 MPa to 200 MPa when hot-drawing with a draw ratio of 2.[31] Alignment of PVA has also been reported for continuously-spun lignin-PVA fibres with 5-50% lignin content, gel-spun from DMSO into methanol/acetone and hot-drawn in four stages at temperatures between 100 °C and 240 °C, generating fibres with tensile strengths of around 0.75 GPa and moduli of around 30 GPa.[32]

This work develops the wet-spinning of lignin-PVA fibres with a lignin content of 75% from an ionic liquid water mixture into a continuous process. Hot-drawing is then applied to induce molecular alignment and reduce the fibre diameter; both factors are expected to improve performance. Since they are coupled, a systematic series of experiments was designed to investigate which is more important for these high lignin content lignin-PVA fibres.

Results and discussion

Continuous wet-spinning of lignin-PVA fibres

The work preceding this study by Yang *et al.* extruded lignin-PVA dope solutions with 75/25 wt%/wt% polymer ratio into a rotating coagulation bath, which used the viscous force of the coagulant (water) to straighten the fibres.[18] Here, wet-spinning of lignin-PVA fibres was performed using a continuous spinning line which generated, on average, 4 m long single filaments which were wound onto spools. In addition to being more relevant to scale-up, continuous spinning has several advantages, for example, longer lengths of more consistent fibres can be produced more quickly. Variation of the ratio between extrusion speed and collection speed may also reduce the fibre diameter and induce some alignment during coagulation. Additional processes, including washing, drawing, heating, and drying can be gradually implemented in-line; however, offline exploration can help to understand the efficacy of each step before combining them.

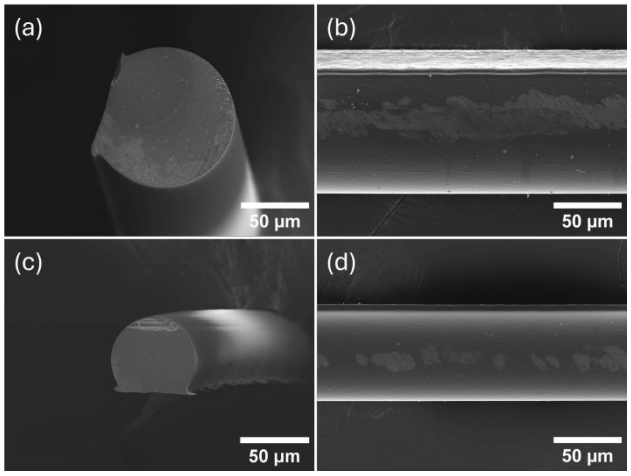

View Article Online
DOI: 10.1039/D5FD00099H

Figure 1. SEM images of air-dried as-spun Kraft lignin-PVA fibres spun continuously from [DMBA][HSO_4] and water mixtures using a 25 G (260 µm) spinneret (a, b) and a 30 G (159 µm) spinneret (c, d).

Extrusion of the lignin-PVA fibres was indeed possible at a faster rate (2.5 mL/h) on the continuous line compared to batch-wise processing used by Yang *et al. (*at 0.6 mL/h). A photo of a fibre that was collected and air-dried on the roll can be seen in the Supplementary Information in Figure S1. Extrusion through two needle spinnerets of different sizes was demonstrated, one with 30 G (inner diameter 159 µm) or 25 G (inner diameter 260 µm). For the lignin-PVA fibres extruded through the smaller diameter (30 G) needle, a maximum relative collection rate of $0.8v_e$ (0.8 times the linear extrusion velocity) was achieved. Faster collection rates resulted in fibre breakage. The 25 G fibres could be collected at faster speeds, at least up to $1.6v_e$, but the take-up rate was maintained at $0.8v_e$ for consistency in this study.

As the fibres were collected on the roll while wet, the circular cross-sections of the lignin-PVA fibres that form during coagulation were not retained after collection. During drying, solvent evaporation from the continuous fibres under tension induced anisotropic shrinkage along the fibre axis, generating normal contact forces at the fibre-roll interface (Figure 1). The flattened shape may affect the fracture mechanics and result in the underestimation of tensile properties, however, trends should not be affected. Including a drying step in the continuous spinning will eliminate the deformation in the future. For commercial applications, carbon fibres are typically circular, but other shapes are also used, for example, so called "kidney bean" fibres used for the Toray M55 grade.

Fibre diameters for the air-dried 30 G and 25 G as-spun fibres were 64 ± 3 µm and 106 ± 5 µm, respectively. These fibre diameters were either similar to or smaller than those obtained by Yang *et al.* (100-120 µm) using a rotating coagulation bath and 27-gauge (210 µm diameter) spinneret for the same dope composition.[18] A similar diameter for different spinnerets suggests that the dope viscosity may have varied between the spinning dopes used in this work and Yang *et al.* (lower viscosities generate smaller fibre diameters). The dope viscosity can be adjusted through the dope composition, using a range of factors such as polymer ratio, the lignin and PVA type, and also dope ageing time.[18, 21] The 25 G and 30 G as-spun fibres had similar tensile strengths (50 ± 9 MPa and 55 ± 6 MPa, respectively), an improvement on the wet-spun fibres produced by Yang *et al.* using a rotating spinning bath, with tensile strengths of around 37 MPa.[18] The moduli of the continuously spun fibres (5.0 ± 0.8 GPa and 4.6 ± 0.2 GPa) were similar to the batch-spun fibres (around 4.8 GPa) reported previously. The estimated carbon yield for the continuously-spun lignin-PVA fibres (38.0%), determined by TGA under nitrogen (Figure S2), matched the estimated carbon yield measured for the Kraft lignin fibres batch wet-spun by Yang *et al.* (36 ± 2.8%).[18]

Hot-drawing

Hot-drawing applies heat to a fibre to increase the mobility of polymers in the material and allow for reorientation of polymer molecules under mechanical tension; elongation tends to lead to improved molecular alignment. Depending on the type of polymer, different temperatures are suitable for hot-drawing. To determine a suitable hot-drawing temperature for the lignin-PVA system, the air-dried as-spun fibres were subjected to hot-drawing over a range of temperatures, using a continuous single fibre processing unit. Temperatures from between 140 and 240 °C in 20 °C increments were investigated. At 200 °C and above, the fibres were deformed due to the evolution of bubbles from within, likely a result of rapid evaporation of water present in the air-dried lignin-PVA blend (4.7 wt%, calculated from the TGA), although water may also be generated by dehydration reactions in the lignin. At temperatures below 180 °C, fibre elongation was observed but the maximum draw ratio (DR) was limited to 12 before the fibres broke. It was found that an exceptionally high DR of 20 was accessible at 180 °C without the occurrence of bubbling, hence this temperature was used for further investigation. The suitability of 180°C as the hot-drawing temperature can be explained with DSC measurements, shown in the SI in Figure S3, which determined a glass transition temperature for the lignin (T_g = 169 °C), and a first melting transition for the PVA (160-200°C, with the peak at 189 °C).

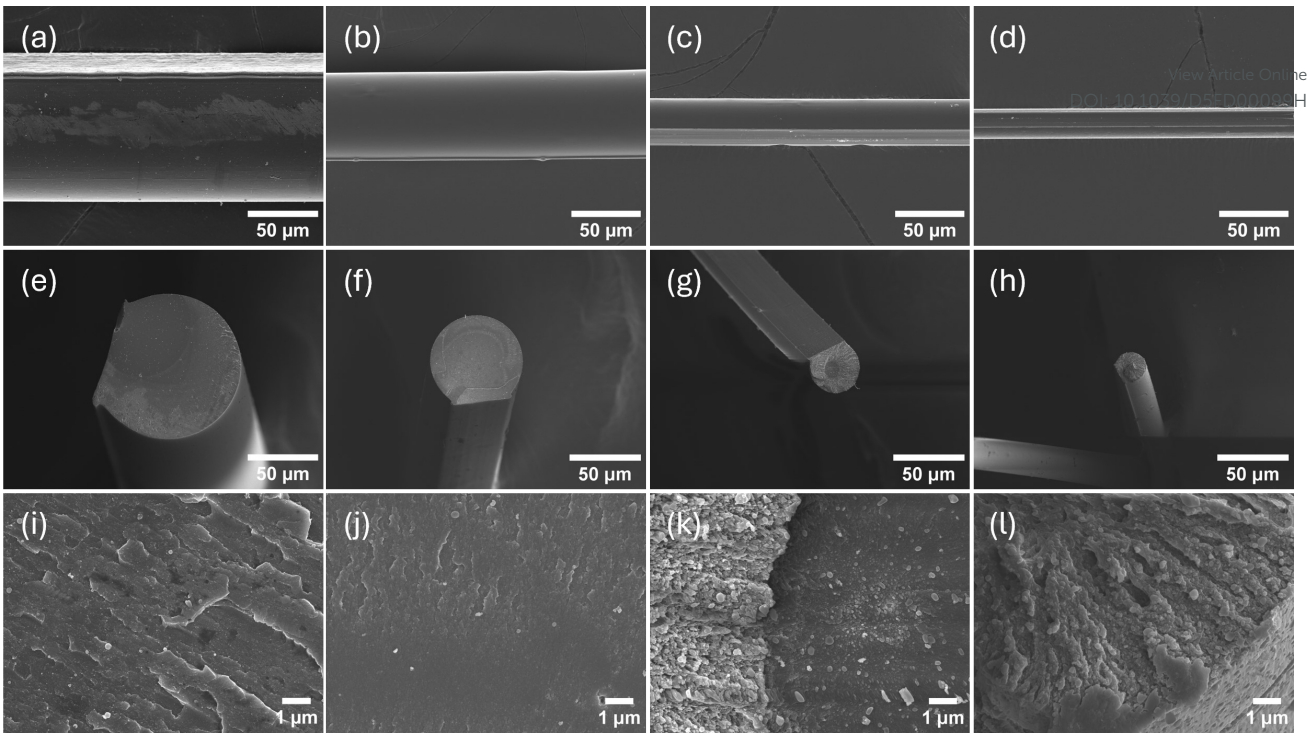

Figure 2. SEM images of the fibre lengths of 25 G as-spun lignin-PVA fibres (a), and hot-drawn fibres at 180 °C to DR 2.5 (b), DR 8 (c), and DR 20 (d). The respective cross-sections are seen at the same magnification (e-h) and at higher magnification (i-l).

SEM images of as-spun and three selected 25 G fibres hot-drawn at 180 °C are shown in Figure 2. The hot-drawn fibres had uniform diameters, with the flattened fibre shapes preserved. The fibre diameters decreased with increasing draw ratio; fibres obtained with DR 20 had a diameter below 30 µm, a more than 3-fold reduction compared to the as-spun fibres. The drawn fibres had smooth surfaces but an increasingly rugged cross-sectional fracture surface. A similar pattern has been observed on the cross sections of hot-stretched polyethylene fibres and is attributed to the formation of fibrillar crystals.[33]

To distinguish between the effect of decreasing fibre diameter and induced polymer orientation on the properties of drawn lignin-PVA fibres, a series of drawing experiments were performed up to the maximum possible draw ratio of 20, with the draw ratios selected to achieve matching diameters for the 30 G and 25 G fibres. Figure 3 shows the relationship between increasing draw ratio and reducing fibre diameter for the hot-drawn fibres. As expected, the fibre diameter scaled with the reciprocal square root of the draw ratio, consistent with the assumption that the fibre volume remains constant during hot-drawing; this assumption is consistent with the finding that mass loss only occurred above 200°C in the TGA of air-dried lignin-PVA fibres (Figure S2).

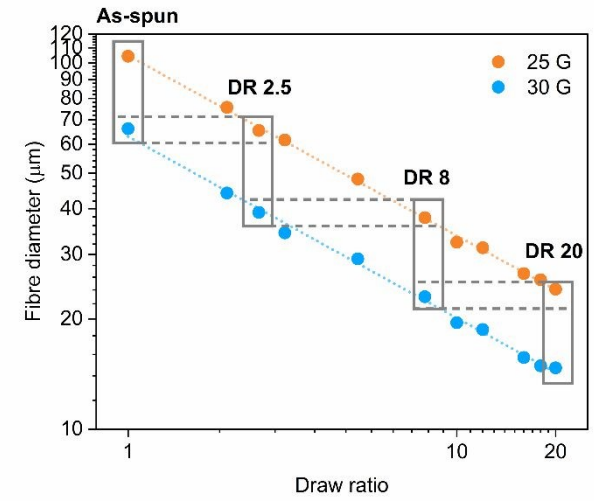

Figure 3. Relationship between fibre diameter and draw ratio (DR) for lignin-PVA fibres extruded through 25 G (260 µm) and 30 G (159 µm) spinnerets. Vertically oriented boxes indicate fibres with the same draw ratio (but different diameter) and horizontally oriented boxes (dashed) indicate hot-drawn fibres with the same diameter (but different draw ratios). The orange and blue lines (dotted) fitted to the 25 G and 30 G data have slopes of -0.49 and -0.50, respectively.

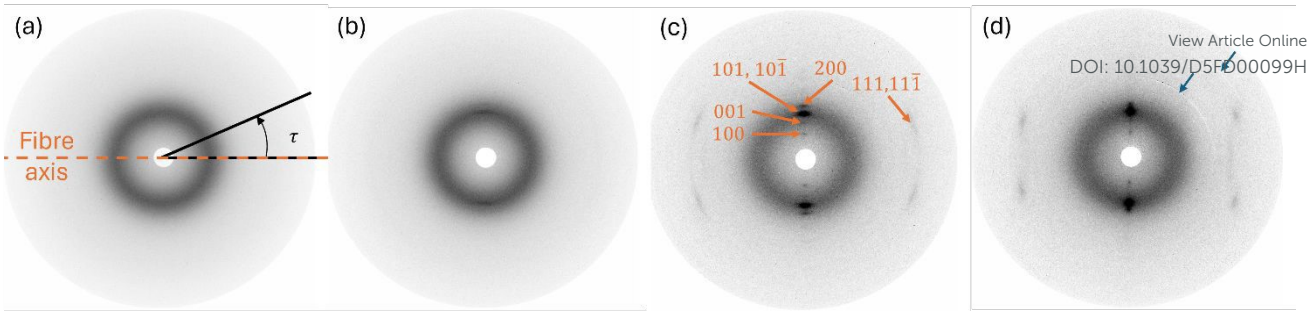

Figure 4. WAXS patterns of 25 G as-spun lignin-PVA fibres (a), and lignin-PVA fibres hot-drawn at 180°C to DR 2.5 (b), DR 8 (c), and DR 20 (d). The blue arrows highlight rings resulting from the background subtraction.

Wide-angle X-ray scattering (WAXS) of hot-drawn fibres

X-ray scattering was employed to inspect the effect of drawing on the orientation of polymers in the lignin-PVA fibres. X-ray scattering images from the hot-drawn lignin-PVA fibres made with 25 G and 30 G spinnerets are shown in Figure 4 and Figure S4 (a-d), respectively. The corresponding scattering diagrams, reporting the measured intensity integrated over the azimuthal angle as a function of the wave-vector Q, are shown in Figure 5 (a) and Figure S5 (a). As with the mechanical properties, the flattened fibre cross section should not affect the interpretation of the WAXS results. For the as-spun fibres, a broad modulation around Q≈1.4 Å^{-1} was observed and assigned to a scattering signal from both lignin (Figure S6) and amorphous PVA, which corresponds to the interchain distance.[27] The most intense scattering signal from amorphous PVA is located around 1.4 Å^{-1}. The scattering diagram of the fibres hot-drawn to DR 8 indicates the presence of crystalline PVA. Its space group is $P2_1/m$, with unit cell parameters a = 7.81 Å, b = 2.52 Å, c = 5.51 Å and γ = 91.7°.[34] The corresponding Bragg peaks, labelled by the three Miller indices hkl are shown in Figure 4 and Figure S4. The $10\bar{1}$ and 101 peaks of crystalline PVA appear at $Q \approx 1.39$ Å^{-1}, i.e. at around the same spacing as the intense peak of amorphous PVA, the chains being aligned along the axis $\vec{b}$ in the crystal. Crystalline PVA was also found for DR 2.5, albeit in smaller amounts, as the peak which includes the adjacent $10\bar{1}$ and 101 peaks at $Q \approx 1.39$ Å^{-1} is visible in Figure 4 (b) and Figure S4 (b). For the highest draw ratio of 20, the $10\bar{1}$ - 101 peak was more intense compared to other h0l peaks, which may indicate supplementary partial crystallisation of PVA.

In Figure 4 (b-d) and Figure S4 (b-d), h0l peaks are located perpendicularly to the fibre axis, around τ values of 90 and 270°. It follows that the crystalline PVA domains present strong preferential orientation with respect to the fibre axis, with axis $\vec{b}$, i.e. the PVA chains, aligned with the fibre axis. The intensities at $Q = (1.39 \pm 0.04)$Å^{-1} as a function of the azimuthal angle τ on the

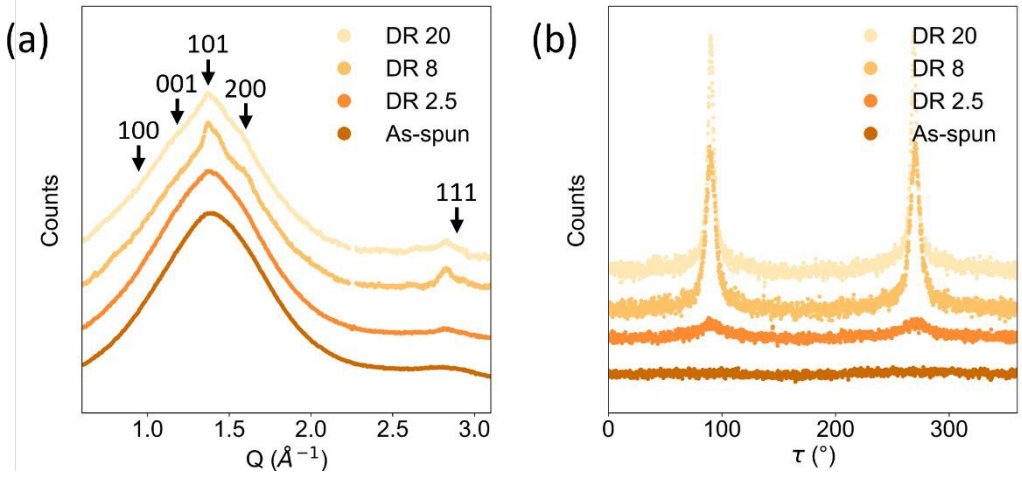

Figure 5. (a) Scattering diagrams and (b) angular modulation of the intensity for the as-spun and hot-drawn 25 G fibres. Curves are translated vertically for the sake of clarity.

detector are reported in Figure 5 (b) and Figure S5 (b). They were fitted by Lorentzian functions (Figure S7) and their full width at half maxima (FWHM) are reported in Table 1. For the as-spun fibre, the broad ring around 1.4 Å^{-1} was slightly modulated. Although both PVA and lignin contribute to the ring, we attribute the angular modulation to a preferred orientation of amorphous PVA, which is a long (Mw ~100 kDa) linear polymer, rather than a preferred orientation of the Kraft lignin, which is mixture of short, disperse macromolecules. Based on the FWHM, the polymer orientation was slightly higher for the fibres spun with the smaller

diameter (30 G) spinneret, which was FWHM=109° vs FWHM=139° for the 25 G spinneret, when having experienced the same drawing conditions. This effect may be due to different shear stresses experienced while extruding the fibre, which was higher for fibres generated with the smaller diameter (30 G).

View Article Online
DOI: 10.1039/D5FD00099H

The FWHMs reported for the hot-drawn fibres reflect the orientation of crystalline PVA after drawing. For the 2.5 draw ratio, the orientation was stronger for the 30 G fibre than for the 25 G fibre (FWHM = 26° vs 31°), which may be a consequence of the increased alignment of amorphous PVA in the as-spun fibres. The orientation increased with the draw ratio, reaching FWHM=6-7° for DR 20. The FWHMs were similar for the 25 G and 30 G fibres for draw ratios of 8 and 20, which shows that the initial conditions of fibre formation are not relevant at high draw ratios. The crystallisation and orientation in pure PVA fibres, with increasing draw ratio, is well documented in the literature.[27, 30, 31]

The amount of oriented polymer in as-spun fibres and in hot-drawn fibres can be considered with respect to the amount of lignin (assumed to be non-oriented due to the molecular shape) and non-oriented PVA. The precise determination requires extensive calculations to move from reciprocal space to direct space, which are beyond the scope of this study.[35] However, it can be estimated by comparing the areas of signals in the reciprocal space after subtracting the signal from the sample to smaller or larger Q-regions than the region of interest. For this relative analysis, the ratio between oriented PVA and non-oriented PVA and lignin for the larger diameter (25 G) fibres was compared to ratio for the smaller diameter (30 G) fibres. The results were as follows: r=1.7 for as-spun fibres, r=1.3 for DR 2.5, r=1.4 for DR 8 and r=1.2 for DR 20 hot-drawn fibres. This comparison suggests that more of the oriented fraction was present in the 25 G fibres than in the 30 G fibres.

In an interesting study on lignin-PVA fibres obtained by gel spinning, Lu *et al.* argued that H-bonding between lignin and PVA allows for the alignment of lignin segments with PVA, which is correlated with the increased mechanical properties.[32] The lignin orientation factor was deduced from Raman anisotropy. It was most important for the 5-95% lignin-PVA fibres but was also present to a lesser extent for 50-50% lignin-PVA fibres. For the 75-25% lignin-PVA fibres generated in this work, using the X-ray scattering method to probe alignment, no lignin alignment was found. Indeed, no noticeable angular modulation of the broad peak in Q around 1.4 $Å^{-1}$ is visible for the DR 20 fibres, as shown by the flat background in Figures S7 (d) and (h).

Table 1. Full Width at Half Maximum (FWHM) for the fitted peaks of the as-spun and hot-drawn fibres spun from 25 G (260 µm) and 30 G (159 µm) spinnerets at different draw ratio (DR).

	FWHM (°)	
	25 G	**30 G**
As-spun	130	89
DR 2.5	31	26
DR 8	10	9
DR 20	6	7

Mechanical properties of hot-drawn fibres

Hot-drawing increased the tensile properties of the lignin-PVA fibres (Figure 6 (a)), with increasing draw ratio resulting in a linear increase in tensile strength. The fibre diameter had an insignificant influence on tensile strength (Figure 6 (b)).

The degree of orientation and the amount of crystalline PVA present in the hot-drawn fibres greatly influenced the mechanical properties. The highest tensile strengths were obtained at DR 20, with around a 5-fold increase over the undrawn lignin-PVA fibres; the similar values of 249 ± 11 MPa (25 G) and 235 ± 26 MPa (30 G) are consistent with the similar degree of molecular alignment observed by WAXS. The tensile moduli exhibited a similarly linear trend with draw ratio, but the fibres spun from larger diameter (25 G) spinneret had a slightly higher modulus across the entire hot-drawing range (Figure 6 (c)). The improved orientation and partial PVA crystallisation in DR 2.5 fibres compared to the as-spun fibres did not manifest as strongly in the tensile properties as for the larger draw ratios. In fact, the tensile modulus for DR 2.5 decreased slightly for both the 25 G and 30 G fibres. The stress-strain behaviour of the lignin-PVA fibres was more ductile after hot-drawing (Figure S8). Overall, higher draw ratios are optimal for a significant improvement in mechanical properties of the lignin-PVA fibres.

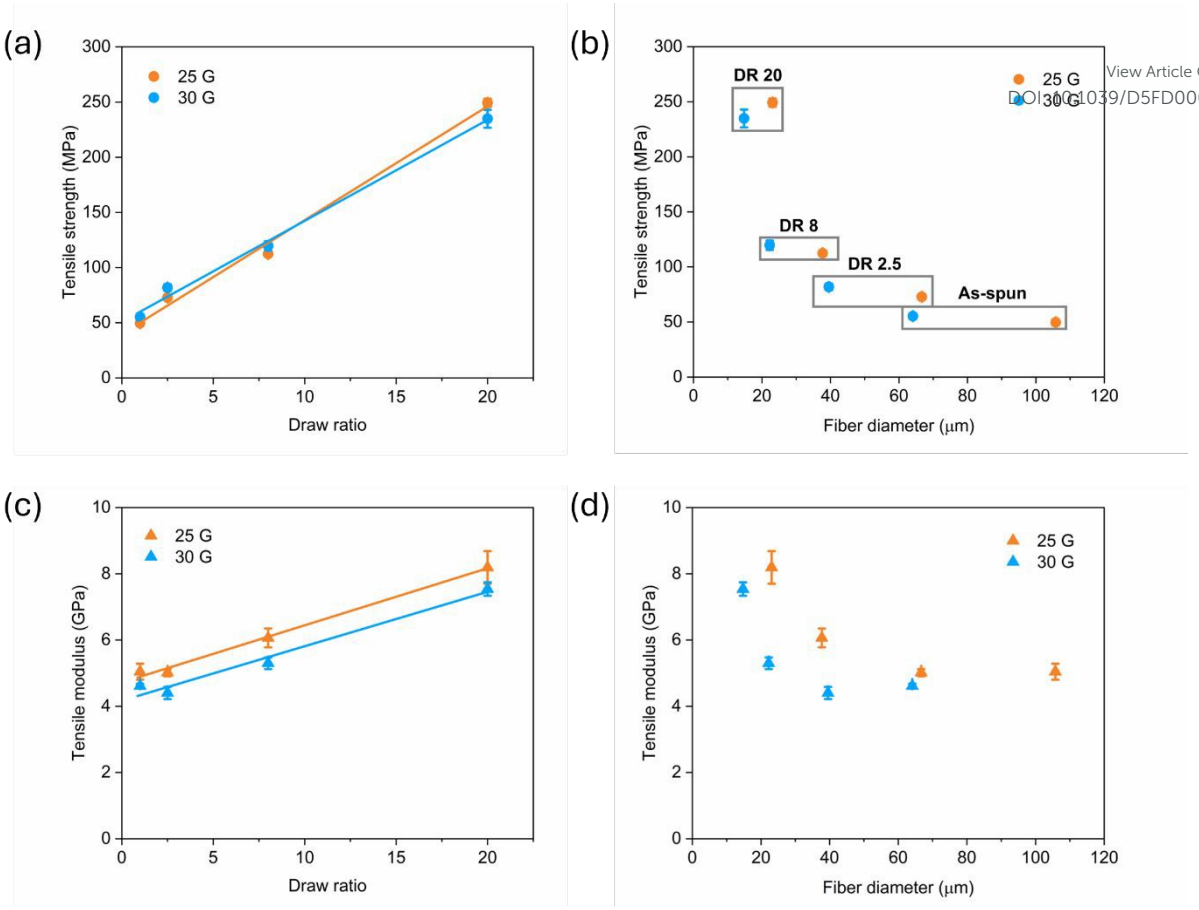

Figure 6. Tensile strength (top) and modulus (bottom) of 25 G and 30 G lignin-PVA fibres hot-drawn to a series of draw ratios.

Stabilising the lignin PVA fibres

The as-spun and hot-drawn fibres were stabilised batch-wise, applying the standard protocol employed by Yang *et al.* which uses slow temperature ramp rates of 1 °C/min from 25 to 100 °C and 0.2 °C/min from 100 to 250 °C in air. Fixed lengths of the as-spun and hot-drawn fibres were stabilised under load to reduce the likelihood of polymer relaxation, especially in the hot-drawn fibres during the slow heating process, which would result in shrinkage in the axial direction with insufficient tension. The fibre diameters were 6-9% smaller after stabilisation under self-induced tension and the non-circular shape of the cross-sections was again preserved (Figure 7). The stabilised fibres were characterised by tensile testing, WAXS and FT-IR spectroscopy.

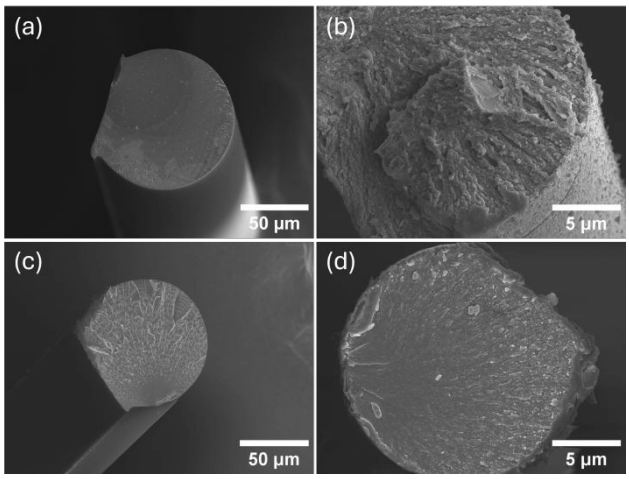

Figure 7. SEM images of an (a) as-spun 25 G fibre, (b) 25 G fibre hot-drawn to DR 20, (c) stabilised 25 G fibre, and (d) 25 G fibre hot-drawn to DR 20 after oxidative stabilisation.

FT-IR spectroscopy of lignin-PVA fibres

FT-IR spectroscopy was used to characterise the chemical functionality in the lignin-PVA blends and assess structural changes in the polymers after stabilisation (Figure 8). The broad absorption peak with maximum at 3274 cm^{-1} was related to the stretching vibration of the OH groups in PVA; there is also a hydroxyl band in the IR-spectrum of the lignin, from the OH groups in lignin and likely a contribution from absorbed water. A relative red shift of the -OH peak maximum to 3257 cm^{-1} for lignin-PVA fibres indicates changes in the hydrogen bonding occurred during blending, suggesting interactions between the PVA and the lignin via hydrogen bonding.[36]

Stabilisation of the lignin-PVA fibres resulted in the loss of bands linked to O-H stretches, C-H stretches in methylene groups, and C-O stretches in alcohols (at 3257 cm^{-1}, 2840-3000 cm^{-1}, and 1030-1260 cm^{-1}, respectively). The C=O stretch at 1690 cm^{-1} which is indicative of aldehydes and carboxylic groups, remained in the stabilised fibre. The more pronounced C=O stretch band is attributed to the oxidation of aliphatic OH groups and has been used as an indicator of successful oxidative stabilisation. More intense C=O and C=C bands were observed for the stabilised fibres with increasing draw ratio (Figure 8 (b)), while there was reduced absorption by methylene and methyl groups, trends that have been observed for stabilised lignin fibres before.[36] A reappearance of C-H stretch at 2930 cm^{-1} for the stabilised fibres was detected with increasing draw ratio, suggesting the formation of new aliphatic motifs.[36]

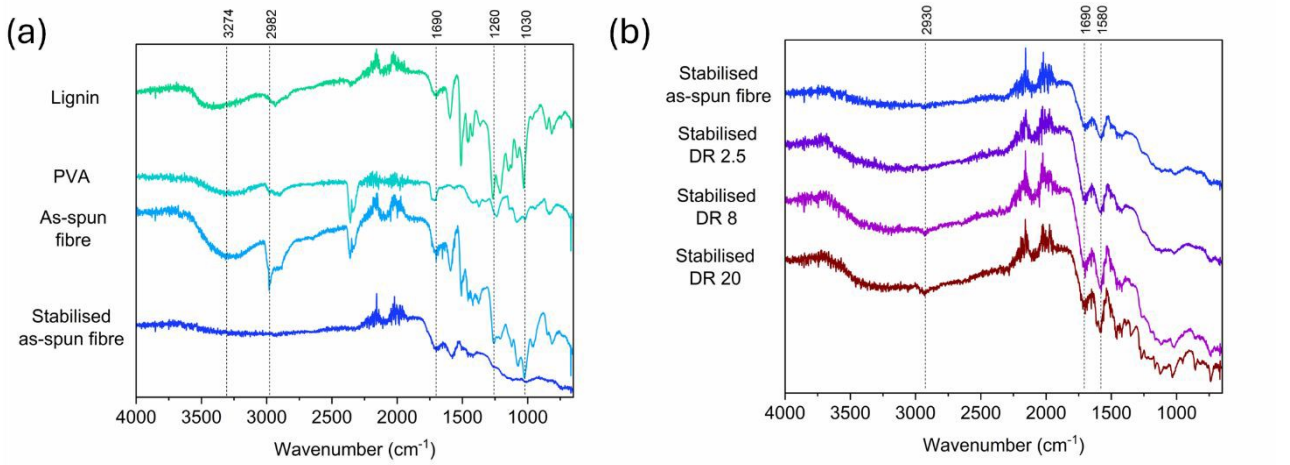

Figure 8. FT-IR spectra of the (a) Kraft softwood lignin, PVA, as-spun lignin-PVA fibres, and stabilised as-spun lignin-PVA fibres, and of (b) stabilised lignin-PVA fibres obtained after hot-drawing with different draw ratios.

Wide-angle X-ray scattering (WAXS) of stabilised hot-drawn fibres

The X-ray scattering images for the thermally stabilised lignin-PVA fibres made with 25 G and 30 G spinnerets are shown in Figure 9 and Figure S4 (e-h), respectively. Their corresponding scattering diagrams can be found in Figure 10 (a) and Figure S5 (c) and the angular dependence of the intensity at $Q = (1.39 \pm 0.04)\text{Å}^{-1}$ is shown in Figure 10 (b) and Figure S5 (d). The images show that the PVA orientation and crystallisation was lost while stabilising the fibres at 250°C, which is ascribed to the mobility of the PVA at this temperature (Figure S3).[28] Unexpectedly, the broad peak related to the local structure of lignin and PVA for the stabilised as-spun fibre widened and shifted to larger Q-values for the stabilised hot-drawn fibres (Figure 10 (a) and Figure S5 (c)). Further analysis is necessary to understand the origin of this effect in terms of the local structure in direct space.

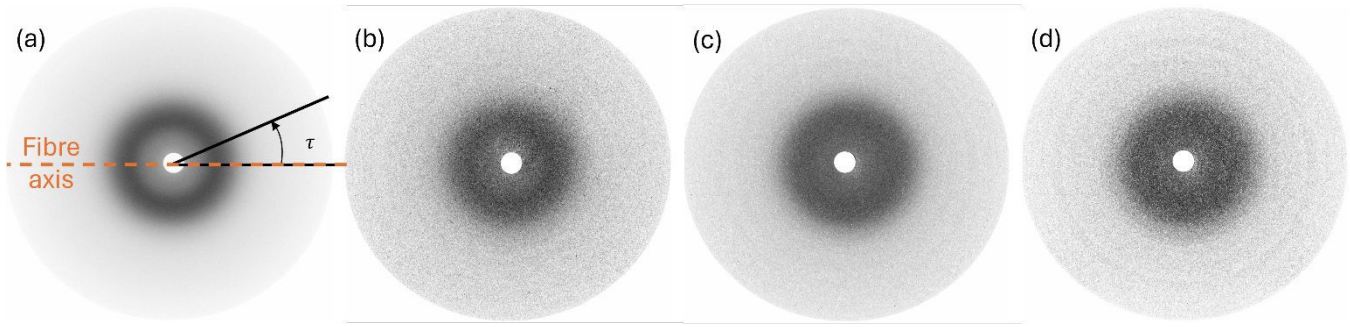

Figure 9. WAXS images of stabilised (a) as-spun, (b) DR 2.5, (c) DR 8, (d) DR 20 lignin-PVA fibres produced from the 25 G spinneret. The smaller the fibre, the weaker the signal, which leads to residual rings around 2.26 $Å^{-1}$ and 3.03 $Å^{-1}$ that persisted in the processed images even after background subtraction.

View Article Online
DOI: 10.1039/D5FD00099H

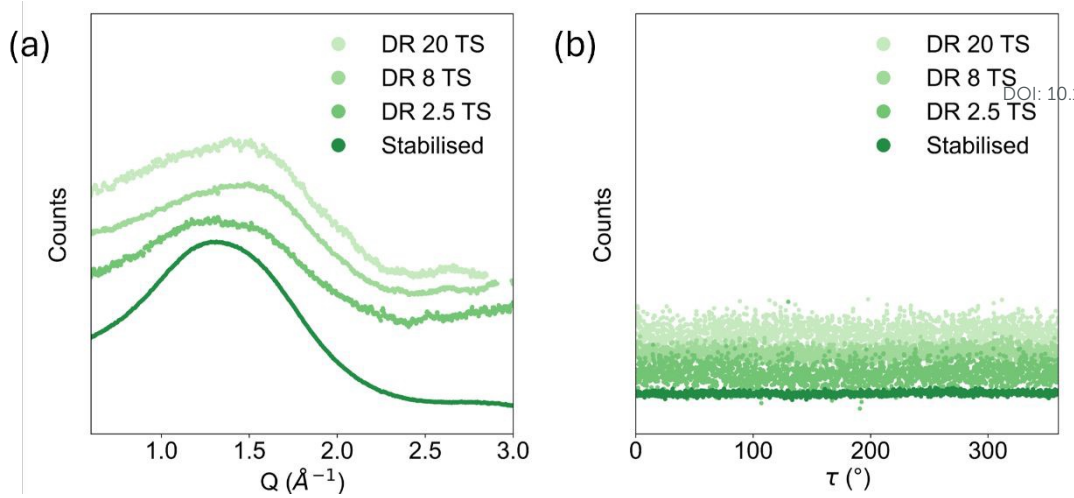

Figure 10. (a) Scattering diagrams and (b) angular modulation of the intensity for the stabilised as-spun and hot-drawn 25 G fibres. Curves are translated vertically for the sake of clarity.

Mechanical properties of stabilised fibres

This study reports for the first time the tensile properties for stabilised ionic liquid spun lignin-PVA fibres. The tensile strengths of the undrawn 25 G and 30 G fibres increased to 105 ± 26 MPa and 124 ± 11 MPa, respectively, around double of the as-spun fibres. Increased crosslinks and healing of fibre defects during the heating ramp may account for the change in behaviour and the increased strength compared to the unstabilised as-spun fibres.

However, increasing tensile strength with increasing draw ratio was no longer observed after fibre stabilisation (Figure 11). The loss of polymer orientation seen with WAXS was mirrored by the mechanical properties of the stabilised fibres, which became similar for all draw ratios. A slight decrease in tensile strength was observed with increasing diameter (Figure 11 (b)) but may not

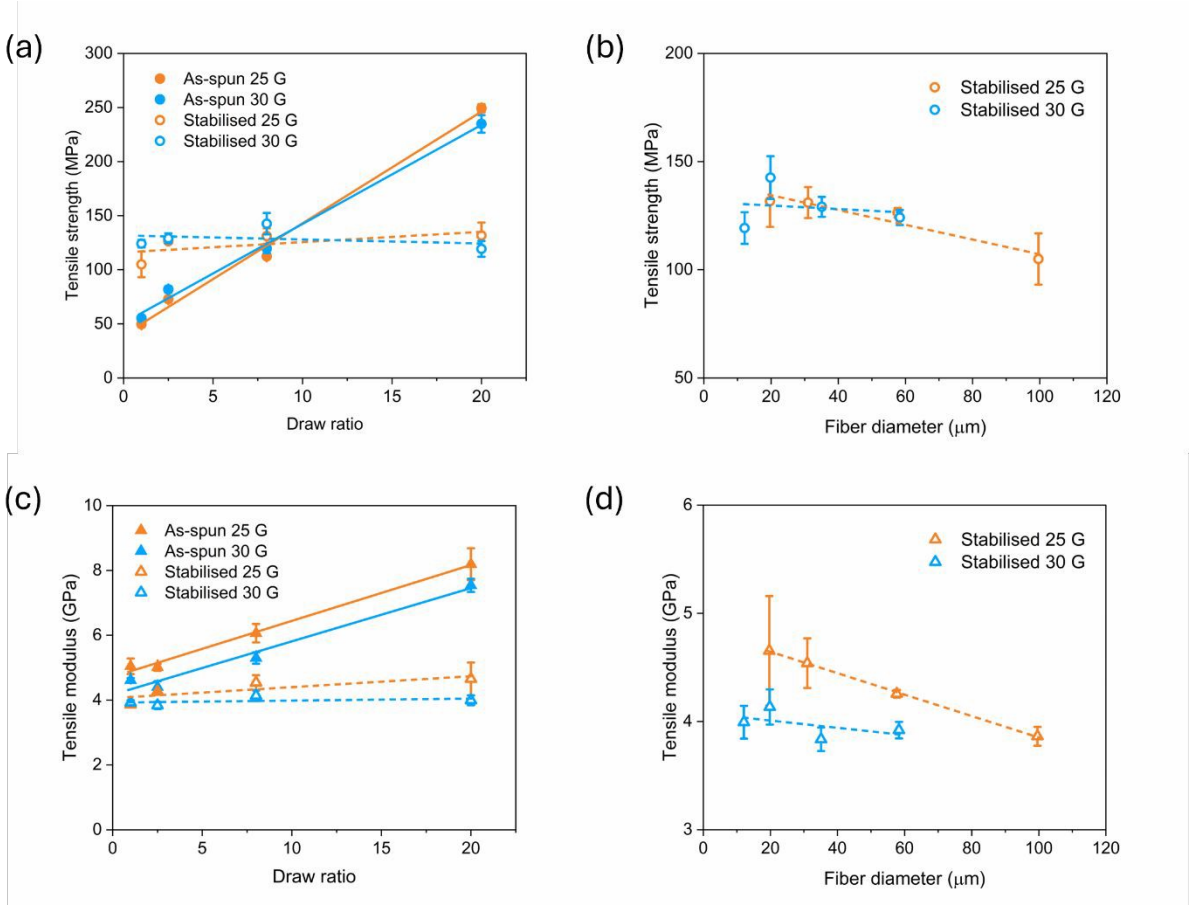

Figure 11. Tensile strength (a and b) and modulus (c and d) of stabilised 25 G and 30 G lignin-PVA fibres hot-drawn to a series of draw ratios against hot-drawn as-spun fibres.

be significant. After stabilisation, the as-spun and hot-drawn fibres displayed similarly shaped stress strain curves, with a significant yield plateau (Figure S8). The moduli of the stabilised hot-drawn fibres were around 3.9 ± 0.2 GPa, similar to those of the as-spun fibres, again consistent with lost polymer orientation. There was a diameter effect for the modulus (Figure 11 (d)), with smaller diameter fibres having a higher tensile modulus.

View Article Online
DOI: 10.1039/D5FD00099H

In summary, using the applied stabilisation conditions, the oriented polymers relaxed before the structure was fixed, which could be responsible for the lack of trend in tensile strength with draw ratio or fibre diameter. A faster temperature rate or additional drawing during stabilisation may be needed to retain the oriented structure.

Experimental

Materials and methods

Softwood Kraft lignin was supplied by the Research Institutes in Sweden (RISE), isolated through the LignoBoost process from black liquor derived from spruce and pine biomass. Poly(vinyl alcohol) (PVA) with an average molecular weight of 85,000 – 124,000 g/mol, 87-89% hydrolysed, was purchased from Sigma Aldrich. The materials were used as received. The ionic liquid (IL) *N,N*-dimethylbutylammonium hydrogen sulfate [DMBA][HSO_4] was synthesised at Imperial College London using *N,N*-dimethylbutylamine (> 99% purity) and sulfuric acid solution (66.3%) purchased from VWR.[18] The acid-to-base ratio of the ionic liquid was confirmed as 1.03 ± 0.01 using an automatic titrator (volumetric Karl Fischer titrator, Mettler Toledo V20) as discussed previously.[18]

Fibre spinning

The dope solution was prepared following the method described in previous work by Yang *et al.*[18] In summary, an aqueous PVA solution was stirred for 1 h at 85 °C followed by the addition of [DMBA][HSO_4] and Softwood Kraft lignin. This dope solution was stirred for 1 h at 60 °C and allowed to cool to room temperature. The final dope composition was 3:1 lignin:PVA at 16% solid loading in a [DMBA][HSO_4]$_{60\%}$ $H_2O_{40\%}$ solvent. The dope solution was extruded from a 2.5 mL Gastight 1000 PTFE Luer lock (TLL) syringe (Hamilton) through ½" needles with two different gauges (25 G and 30 G with inner diameters of 260 and 159 µm respectively) using a high-pressure syringe pump (Chemyx Fusion 6000X) at an extrusion rate of 2.5 mL/h. The fibres were allowed to coagulate in a deionised water bath for an average residence time of at least 45 s and collected on a Delrin acetal roll (48 mm diameter) at 0.8 times the take-up speed relative to the linear extrusion velocity. The rolls were operated by stepper motors controlled by IC drivers (TMC2130, Trinamic) and a microcontroller (Arduino Uno) constructed at Imperial College London (winding unit). The fibres were allowed to air-dry on the roll. The wet-spinning parameters are detailed in the supplementary Table S2.

Hot-drawing

The air-dried fibres were hot-drawn through a 30 cm ceramic-insulated heating zone on the conditioning unit of a microfiber line (Xplore), adapted with two Delrin acetal rolls and their stepper motors as feed-in and take-up rolls. The fibres were hot-drawn at a feed-in rate of 15 cm/min to a series of draw ratios (DR 2.5, 8, and 20), where DR is a multiplier of the feed-in rate for the take-up rate (Table 2).

Table 2. Parameters for hot-drawing lignin-PVA fibres through a 32 cm heating zone.

Draw ratio	Feed in rate, cm/min	Take-up rate, cm/min
2.5	15.1	37.7
8	15.1	120.6
20	15.1	301.6

Oxidative stabilisation

The air-dried and hot-drawn fibres were fixed onto graphite frames with a gauge length of 19 cm using Glassbond Aluseal Adhesive Cement No.2 ceramic paste and oxidatively stabilised in a Memmert UNP-200 oven following the temperature program of 1 °C/min from 25 °C to 100 °C, 0.2 °C/min from 100 °C to 250 °C, holding at 250 °C for 1 hour before ambient cooling to room temperature.

Scanning electron microscopy (SEM)

The fibres were fractured and secured on aluminium stubs with carbon tape and coated with 10 nm of Chromium. The fibre lengths and cross-sections were observed using a Zeiss Gemini Sigma 300 scanning electron microscope using the InLens detector with an accelerating voltage of 5 kV and an aperture of 30 µm at a working distance of 6 mm.

Wide-angle X-ray scattering (WAXS)

View Article Online
DOI: 10.1039/D5FD00099H

Wide angle X-ray Scattering (WAXS) measurements were performed on a rotating anode X-ray generator (MicroMax 007, Rigaku Corp., Japan; 40 kV-16 mA) of the MORPHEUS platform at Laboratoire de Physique des Solides. The X-ray beam was monochromatised and collimated by a multilayer optics (FOX3D 14-39, Xenocs, France) at the copper Kα radiation (λ = 1.5418 Å) with a beam size around 1 mm^2.

Experiments on fibres were performed with the sample placed in a vacuum chamber, to minimise contamination due to air scattering. 2D-WAXS diagrams were collected on a MAR345 detector (marXperts GmBH, Germany) with a 150 µm pixel size, placed behind the vacuum chamber outlet window, at a distance of 148 mm from the sample. The exposure time for each measurement was 2 hours, repeated multiple times for the small diameter fibres. Additionally, several background images were acquired without a sample for the same duration. The final images were added and subtracted by the same number of background images.

The experiment on lignin powder was performed under air, with the powder placed in a borosilicate capillary with a diameter of 0.9 mm. The sample-to-detector distance was 200 mm. A background image taken with an empty capillary was also subtracted.

To plot the scattering diagrams, the final images were integrated over the azimuthal angle on the detector, which provided the intensity as a function of the reciprocal scattering wave-vector Q. Furthermore, the intensities on the scattering diagrams were corrected of the polarisation of X-rays and the geometrical factor of the planar detector. Angular intensity profiles were also plotted, showing the intensity changes integrated over a specific narrow wave-vector range around the wave-vector value of interest, plotted against the azimuthal angle on the detector.

Mechanical testing

Single filaments of the air-dried, hot-drawn, and stabilised lignin-PVA fibres were mounted on card templates for tensile testing with a gauge region of 15 mm. A minimum of 10 samples per set of fibres were tested, and 15 random points along each fibre were measured for an average diameter for each fibre sample using ImageJ applied to images taken on a Leica DM2500 optical microscope with a Basler Ace acA1920 camera. The ends were fixed using Araldite Rapid epoxy and left to cure at room temperature for 10 days before being tested. A minimum of 10 tests were conducted on each fibre, and the fibres were mechanically tested using a Linkam Scientific MFS fitted with a 20 N load cell at 1 mm/min until failure at ambient temperature. The measurements were performed, and the data was processed, following ISO 11566:1996.

Differential scanning calorimetry (DSC)

Differential scanning calorimetry (DSC) was performed to determine the melting transitions of lignin, PVA, and lignin-PVA fibres for hot-drawing. Each sample ranging from 3-7 mg was heated from 25 to 200 ℃ at a rate of 10 ℃/min, cooled to 25 ℃ and heated again to 200 ℃ at the same rate under a nitrogen atmosphere (20 mL/min) using a TA Q2000 DSC (TA Instruments).

Thermogravimetric analysis (TGA)

Thermogravimetric analysis (TGA) was performed using a Pyris 1 TGA (PerkinElmer) to determine the mass loss events for lignin, PVA, and lignin-PVA fibres. The sample was placed on a pre-tared high temperature platinum TGA pan, and the sample was heated from 25 to 900 ℃ at 10℃/min under a nitrogen atmosphere (20 mL/min), with an isothermal step at 100℃ for 30 minutes. The mass loss curves were plotted for the temperature range of 100-900℃.

FTIR-ATR spectroscopy

Attenuated total reflectance Fourier-transform infrared spectroscopy (FTIR-ATR) was used to investigate changes to the chemical bonding in as-spun and hot-drawn lignin-PVA fibres during blending and after stabilisation using a Cary 630 FTIR Spectrometer (Agilent). For each measurement, 16 scans were recorded over the spectral range 4000-650 cm^{-1} at a resolution of 2 cm^{-1}. The spectra were baselined and the 1435 cm^{-1} C-H peak was used as the reference band to normalise the IR absorbance spectra.

Conclusions

Lignin-PVA fibres with a high lignin content (75%) were successfully wet-spun using a low-cost ionic liquid water mixture, using a continuous laboratory scale spinning line, which developed a previously used batch method. The continuous arrangement is well suited to further development to include more extensive in-line washing, gel-drawing, hot-drawing, and drying processes, compatible with conventional industrial scale-up. The possibility of applying drawing was investigated by applying offline hot drawing. Exceptionally high draw ratios, up to 20, were successfully applied, reducing the fibre diameters from 64-106 µm to 15-23 µm, which is a promising range for the diameter scales used for commercial carbon fibre production.

The hot-drawing enhanced the orientation and crystallisation of the PVA phase, which was accompanied by increases in tensile strength. The tensile strength increases were predominantly related to draw ratio, with the highly drawn fibres (DR 20) achieving five times the tensile strength of the as-spun fibres. However, the slow heating rate and possibly the long hold time during the applied oxidative stabilisation resulted in the loss of polymer orientation, and the tensile properties of stabilised fibres were similar and independent of draw ratio. Stabilisation of softwood Kraft lignin can be performed at faster heating rates with a lower holding

time,[37] therefore stabilising the hot-drawn fibres at a faster heating rate could be beneficial to lock in the oriented PVA crystallite structure. Additionally applying stretching at temperatures closer to those needed for stabilisation while avoiding water evolution through more rigorous drying, could contribute to retaining an oriented microstructure during stabilisation.[25] If the molecular orientation in the lignin PVA can be retained through stabilisation and onwards to carbonisation, the mechanical properties of the resulting sustainable low-cost carbon fibres should be improved.

View Article Online
DOI: 10.1039/D5FD00099H

Author contributions

ET and JPFN contributed to this study with methodology, investigation, formal analysis of the experimental lignin-PVA fibre work, visualisation, and writing the original draft. LD contributed to this study with investigation and formal analysis of WAXS experiments, visualisation, and writing of the original draft. SR contributed with methodology by designing and installing the vacuum diffusion chamber for the WAXS studies. PL, MS and ABT contributed to this study with the conceptualisation, funding acquisition, project administration, supervision and writing (review and editing).

Conflicts of interest

There are no conflicts to declare.

Data availability

The data supporting this article have been included as part of the Supplementary Information.

Acknowledgements

The authors thank Dr Charles Shaw for assistance with DSC measurements. The work was funded by the EPSRC and SFI Centre for Doctoral Training in Advanced Characterisation of Materials (EP/S023259/1), the Royce Industrial Collaboration Programme (reference EHZ2494092, ICP311) and the UKRI Impact Acceleration Account (EP/X52556X/1, PSO395) for funding the work. Enny Tran and Lucie Diéval acknowledge the funding of the joint CNRS-Imperial College PhD project 'Spinning sustainable carbon fibres for the energy transition'.

Notes and references

1. J. Zhang, G. Lin, U. Vaidya and H. Wang, *Composites Part B: Engineering*, 2023, **250**, 110463.
2. E. Frank, L. M. Steudle, D. Ingildeev, J. M. Spörl and M. R. Buchmeiser, *Angewandte Chemie International Edition*, 2014, **53**, 5262-5298.
3. P. Gutmann, J. Moosburger-Will, S. Kurt, Y. Xu and S. Horn, *Polymer Degradation and Stability*, 2019, **163**, 174-184.
4. T. Peijs, R. Kirschbaum and P. J. Lemstra, *Advanced Industrial and Engineering Polymer Research*, 2022, **5**, 90-106.
5. D. Choi, H.-S. Kil and S. Lee, *Carbon*, 2019, **142**, 610-649.
6. L. Yan, H. Liu, Y. Yang, L. Dai and C. Si, *Carbon Energy*, 2025, **7**, e662.
7. S.-C. Sun, Y. Xu, J.-L. Wen, T.-Q. Yuan and R.-C. Sun, *Green Chemistry*, 2022, **24**, 5709-5738.
8. A. Bengtsson, J. Bengtsson, C. Olsson, M. Sedin, K. Jedvert, H. Theliander and E. Sjöholm, 2018, **72**, 1007-1016.
9. M. P. Vocht, A. Ota, E. Frank, F. Hermanutz and M. R. Buchmeiser, *Industrial & Engineering Chemistry Research*, 2022, **61**, 5191-5201.
10. Toray Composite Materials America Inc., *T300 standard modulus carbon fiber datasheet*, 2025.
11. J. Ralph, C. Lapierre and W. Boerjan, *Current Opinion in Biotechnology*, 2019, **56**, 240-249.
12. S. Rawat, A. Kumar and T. Bhaskar, *Current Opinion in Green and Sustainable Chemistry*, 2022, **34**, 100582.
13. A. Brandt-Talbot, F. J. V. Gschwend, P. S. Fennell, T. M. Lammens, B. Tan, J. Weale and J. P. Hallett, *Green Chemistry*, 2017, **19**, 3078-3102.
14. P. Tomani, *CELLULOSE CHEMISTRY AND TECHNOLOGY*, 2010, **44**, 53-58.
15. D. A. Baker and T. G. Rials, *Journal of Applied Polymer Science*, 2013, **130**, 713-728.
16. M. Zhang and A. A. Ogale, *Carbon*, 2014, **69**, 626-629.
17. J. Jin, J. Ding, A. Klett, M. C. Thies and A. A. Ogale, *ACS Sustainable Chemistry & Engineering*, 2018, **6**, 14135-14142.
18. S. M. Yang, M. S. P. Shaffer and A. Brandt-Talbot, *ACS Sustainable Chemistry & Engineering*, 2023, **11**, 8800-8811.
19. M. Morales, DOI: 10.3929/ethz-a-010797794, ETH Zurich, 2016.
20. L. Chen, M. Sharifzadeh, N. Mac Dowell, T. Welton, N. Shah and J. P. Hallett, *Green Chemistry*, 2014, **16**, 3098-3106.
21. S. M. Yang, R. I. Muazu, E. Tran, C. B. Talbot, N. Shah, M. S. P. Shaffer and A. Brandt-Talbot, *RSC Sustainability*, 2025, DOI: 10.1039/D5SU00218D.
22. R. Moreton and W. Watt, *Nature*, 1974, **247**, 360-361.

23. D. J. Johnson, *Journal of Physics D: Applied Physics*, 1987, **20**, 286-291.
24. H. Lee, L.-W. Lee, S.-W. Lee, H.-I. Joh, S.-M. Jo and S. Lee, 2014, **14**, 217-224.
25. Y. Luo, M. E. A. Razzaq, W. Qu, A. A. B. A. Mohammed, A. Aui, H. Zobeiri, M. M. Wright, X. Wang and X. Bai, *Green Chemistry*, 2024, **26**, 3281-3300.
26. M. Vaughan, A. Beaucamp and M. N. Collins, *Composites Part B: Engineering*, 2025, **292**, 112024.
27. Q. Wu, N. Chen, L. Li and Q. Wang, *Journal of Applied Polymer Science*, 2012, **124**, 421-428.
28. Q. Wu, N. Chen and Q. Wang, *Journal of Polymer Research*, 2010, **17**, 903-909.
29. C.-A. Link, K.-S. Hwang and C.-H. Lin, *Journal of Polymer Research*, 1994, **1**, 215-219.
30. K.-S. Hwang, C.-A. Lin and C.-H. Lin, *Journal of Applied Polymer Science*, 1994, **52**, 1181-1189.
31. M. Föllmer, S. Jestin, W. Neri, V. S. Vo, A. Derré, C. Mercader and P. Poulin, *Advanced Sustainable Systems*, 2019, **3**, 1900082.
32. C. Lu, C. Blackwell, Q. Ren and E. Ford, *ACS Sustainable Chemistry & Engineering*, 2017, **5**, 2949-2959.
33. Z. Wang, M. An, H. Xu, Y. Lv, F. Tian and Q. Gu, *Polymer*, 2017, **120**, 244-254.
34. C. W. Bunn, *Nature*, 1948, **161**, 929-930.
35. V. Pichot, S. Badaire, P. A. Albouy, C. Zakri, P. Poulin and P. Launois, *Physical Review B*, 2006, **74**, 245416.
36. J. L. Braun, K. M. Holtman and J. F. Kadla, *Carbon*, 2005, **43**, 385-394.
37. I. Norberg, Y. Nordström, R. Drougge, G. Gellerstedt and E. Sjöholm, *Journal of Applied Polymer Science*, 2013, **128**, 3824-3830.

The data supporting this article have been included as part of the Supplementary Information.

View Article Online
DOI: 10.1039/D5FD00099H